Journal of Hazardous Materials 169 (2009) 697–702

Contents lists available at ScienceDirect

Journal of Hazardous Materials

journal homepage: www.elsevier.com/locate/jhazmat

Preparation of alumina–iron oxide compounds by gel evaporation method and its simultaneous uptake properties for Ni^{2+}, NH_4^+ and $H_2PO_4^-$

Fahmida Gulshan, Yoshikazu Kameshima, Akira Nakajima, Kiyoshi Okada*

Department of Metallurgy and Ceramics Science, Tokyo Institute of Technology, O-okayama, Meguro, Tokyo 152-8552, Japan

ARTICLE INFO

Article history:
Received 27 October 2008
Received in revised form 2 April 2009
Accepted 2 April 2009
Available online 9 April 2009

Keywords:
Iron oxide
Alumina addition
Magnetic property
Ion adsorption

ABSTRACT

Fe_2O_3/Al_2O_3 powders with a range of Fe/Al compositions were prepared by a gel evaporation method to investigate the effect of alumina on the product phases, magnetic properties and simultaneous adsorption of Ni^{2+} (a model heavy metal cation), NH_4^+ (a model eutrophication-related cation) and $H_2PO_4^-$ (a model harmful anion). Precursor gels were prepared by dissolving $Fe(NO_3)_3{\cdot}9H_2O$ and $Al(NO_3)_3{\cdot}9H_2O$ in ethylene glycol, evaporating to dryness, grinding and heating at 300–1000 °C for 5 h. The crystalline products were γ-Fe_2O_3 (maghemite), formed at 300–600 °C, or α-Fe_2O_3 (hematite) and $AlFeO_3$, formed >600 °C. The temperatures of the phase change from γ-Fe_2O_3 to α-Fe_2O_3 increased with increasing alumina additions. The resulting lattice parameters suggest that Al^{3+} is incorporated into these phases up to about 15 mol.% at 300 °C, falling to 11 mol.% in the γ-Fe_2O_3 formed at 600 °C. The α-Fe_2O_3 formed at 700 °C contained 6 mol.% Al, increasing to 14 mol.% at 1000 °C. The magnetic properties of the samples were measured using a vibrating sample magnetometer. The saturation magnetization values of the γ-Fe_2O_3-containing samples increased with the addition of alumina to a maximum value of 61 emu/g in the sample containing 95 mol.% Fe_2O_3 heated at 400 °C. The simultaneous adsorption of Ni^{2+}, NH_4^+ and $H_2PO_4^-$ from water was investigated by a batch method. The highest adsorption values were found for the sample containing 80 mol.% Fe_2O_3 heated at 600 °C, which contained both γ-Fe_2O_3 and α-Fe_2O_3. It was therefore concluded that the addition of alumina to iron oxide affects the crystalline phases and phase changes, and enhances the simultaneous cation and anion uptake ability of the materials.

1. Introduction

Recently, the pollution of wastewater and surface water by toxic ions has become a severe environmental problem. The vast majority of toxic ions are waste products of various industrial processes, especially the effluent from electroplating plants, metal finishing operations, mining and mineral processing, oil refining and extractive metallurgy processes. Contamination of water is principally by two types of ions, namely, heavy metal ions, and ions such as ammonium and phosphate which cause eutrophication. A variety of methods have been used to remove toxic ions from water and wastewater, arising from many years of development of absorption technology. Many different adsorbents for wastewater treatment have been commercialized or are being developed [1]. For instance, zeolites and layered double hydroxides (LDHs) are excellent sorbents for cations and anions, respectively, but compounds capable of simultaneously absorbing both cations and anions are preferable for practical use [2]. Previously the effectiveness of amorphous $CaO–Al_2O_3–SiO_2$ (CAS) [3] and $CaO–Fe_2O_3–SiO_2$ (CFS) compounds [4] for simultaneous uptake of both cations and anions has been reported. Such simultaneous ion uptake is thought to be due to a combination of three chemically different components, i.e. the anion exchange property of CaO, the amphoteric properties of Al_2O_3 and Fe_2O_3, and the cation exchange property of SiO_2.

Fe- and Al-hydroxides and oxides are well known to show high uptake of anions [5], especially toxic oxyanions such as arsenate [6,7] and phosphate [8–10]. Chubar et al. [11] synthesized $Fe_2O_3{\cdot}Al_2O_3{\cdot}xH_2O$ with high specific surface area (c.a. 400 m^2/g) by a hydrothermal method; this product showed good uptake of phosphate ions. Tanada et al. [12] investigated adsorption characteristics of phosphate onto aluminium oxide hydroxide from seawater. Hu et al. [13] showed that nanosize maghemite (γ-Fe_2O_3) was very effective in adsorbing Cr^{6+}, Cu^{2+} and Ni^{2+} from wastewater. Li et al. [14] synthesized $Fe_2O_3–Al_2O_3$ compounds by coprecipitation and investigated their photocatalytic functions. The highest photocatalytic decomposition rate of bisphenol A was found in the compound of 90 mol.% Fe_2O_3 composition, illustrating the effect of Al^{3+} incorporation. El-Sharkawy et al. [15] prepared $Fe_2O_3–Al_2O_3$ compounds by coprecipitation and examined their catalytic activity, reporting that the texture, acidic properties and catalytic activity depended on the thermal treatment and Fe_2O_3/Al_2O_3 ratios of the compounds. It is therefore of interest to investigate the effect of Al^{3+} substitution

* Corresponding author. Tel.: +81 357342524; fax: +81 357343355.
E-mail address: okada.k.ab@m.titech.ac.jp (K. Okada).

0304-3894/$ – see front matter © 2009 Elsevier B.V. All rights reserved.
doi:10.1016/j.jhazmat.2009.04.009

for Fe_2O_3 in the Fe_2O_3–Al_2O_3 system on the simultaneous uptake of ions by these compounds. Moreover, some phases of iron oxide have good magnetic properties, suggesting the possibility of combining their adsorption properties with the magnetic separation of harmful components from a polluted system by applying a simple magnetic field. This could replace the common technology of filtration and centrifuge separation, and after magnetic separation, the harmful components could be easily removed from the magnetic particles that could then be reused.

In this study, Fe_2O_3–Al_2O_3 compounds with various Fe/(Fe + Al) molar ratios were synthesized by a gel evaporation (GE) method [16] and tested for the simultaneous removal of harmful ions from wastewater. Here, Ni^{2+} was used as the model for heavy metal ions, NH_4^+ the model for ions implicated in eutrophication and $H_2PO_4^-$ the model for harmful oxyanions. To determine the feasibility of magnetic separation of these compounds, their magnetic properties were also measured. Thus, the objective of this study was to examine the effect of Al_2O_3 additions on the compounds formed, their magnetic properties and their simultaneous adsorption of cations and anions, and also to assess the performance of Fe_2O_3–Al_2O_3 compounds for the simultaneous removal of harmful ions from contaminated water considering as a candidate material for low cost, harmless and high efficiency simultaneous removal of harmful ions.

2. Experimental

2.1. Synthesis of the samples

Fe_2O_3–Al_2O_3 compounds were synthesized by the Pechini process [16] using metal nitrates and ethylene glycol as the starting materials, described here as the gel evaporation (GE) method. The starting materials (ferric nitrate $Fe(NO_3)_3{\cdot}9H_2O$ and aluminium nitrate $Al(NO_3)_3{\cdot}9H_2O$) were dissolved in ethylene glycol at a molar ratio of (total metal nitrates):(ethylene glycol) = 1:3 with the addition of a minimum volume of water to dissolve the nitrates. The resulting solution was warmed on a hotplate stirrer at 90 °C to evaporate the solvents, after which the nitrate–glycol mixture auto ignited, producing voluminous foam and finally yielding a loose powder. The powders were dry-ground in a planetary ball mill (LAPO-1, Ito Seisakusho Ltd., Japan) using a Si_3N_4 pot with 30 Si_3N_4 balls (5 mm ϕ) at 300 rpm for 3 h with a ball: sample mass ratio of 30:1. After grinding, the samples were calcined at 300–1000 °C in air for 5 h at a heating rate of 10 °C/min. In this way, samples containing 0, 20, 40, 60, 70, 80, 90, 95 and 100 mol.% Fe_2O_3 were prepared.

2.2. Characterization methods

X-ray powder diffraction (XRD) patterns were obtained (XRD-6100, Shimadzu) using monochromated Cu Kα radiation (40 kV to 30 mA). The lattice parameters of the crystalline phases were calculated by the least-squares method. The specific surface area (S_{BET}) of the samples was determined by a multipoint BET method using N_2 as the adsorbate (Autosorb-1, Quantachrome). The magnetic properties were determined using vibrating sample magnetization (VSM) equipment (BHV-50H, Riken Electronics) with a powder cell.

2.3. Uptake experiments

Simultaneous uptake of Ni^{2+}, $H_2PO_4^-$ and NH_4^+ was determined at room temperature for 24 h by a batch method using a solution containing 8 mM each of $NiCl_2{\cdot}6H_2O$ and $NH_4H_2PO_4$. The sample/solution ratio was fixed at 0.1 g/50 ml. The pH was measured immediately prior to placing the sample into the solution (initial pH) and after the reaction (final pH). After the uptake experiments, the samples were filtered, washed 3 times with distilled water and dried at 80 °C overnight. The concentrations of Ni^{2+}, $H_2PO_4^-$, Fe^{3+} and Al^{3+} before and after the experiments were analyzed by ICP-OES (Prodigy, Leeman Labs.) while the NH_4^+ concentration was determined by ion chromatography (IA-200, TOA-DKK). The uptake % and uptake (mmol/g) were calculated using the following formulas:

$$\text{uptake (mmol/g)} Q_0 = \frac{(C_i - C_f)V}{M}$$

$$\text{uptake \%} = 100\frac{C_i - C_f}{C_i}$$

where C_i, C_f, V and M are the initial concentration (mmol/L), final concentration (mmol/L), volume of solution (L) and mass of sample (g), respectively.

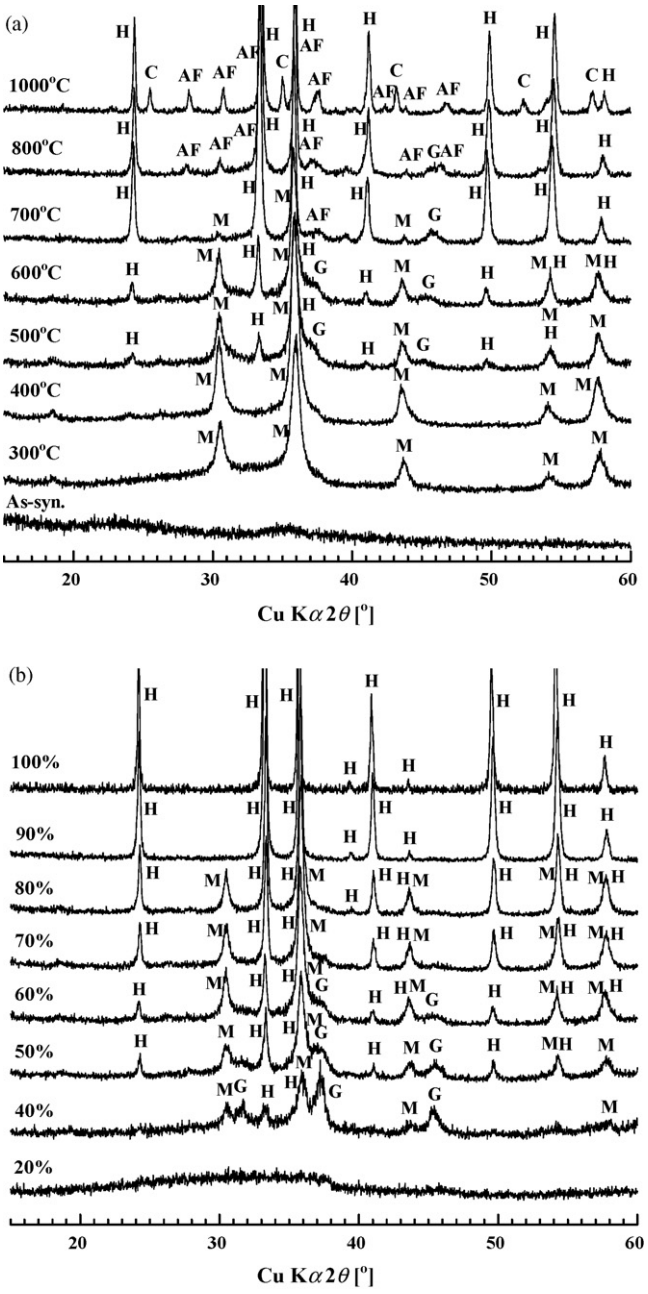

Fig. 1. XRD patterns of (a) samples containing 60 mol.% Fe_2O_3 heated at various temperatures, (b) samples heated at 600 °C with various Fe/(Fe + Al) ratios. Key: AF = $AlFeO_3$, C = α-Al_2O_3, G = γ-Al_2O_3, H = α-Fe_2O_3 and M = γ-Fe_2O_3.

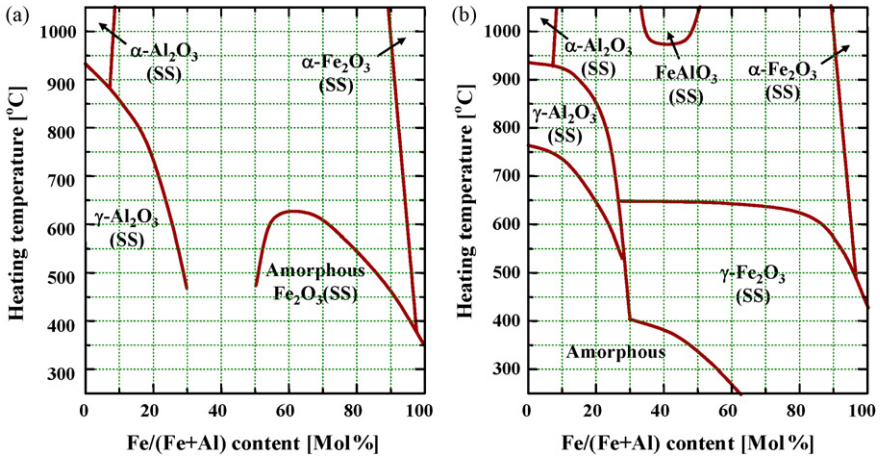

Fig. 2. Field maps of the phases formed in the samples as functions of composition and heating temperature. (a) Samples synthesized by coprecipitation [11] and (b) samples synthesized by the gel evaporation method.

3. Results and discussion

3.1. Effect of alumina on the sample phases

After calcination at 300–1000 °C the crystalline phases in the samples were determined from the XRD patterns using the relevant ICDD data to investigate the structural changes caused by the thermal treatment and by changing the Fe/(Fe + Al) molar ratio. The XRD patterns of the samples are shown in Fig. 1 as a function of heating temperature (Fig. 1(a)) and Fe_2O_3 content (Fig. 1(b)). The as-synthesized samples are amorphous. Fig. 1(a) shows that the samples heated at 300 and 400 °C contain only maghemite (γ-Fe_2O_3). Hematite (α-Fe_2O_3) and γ-Al_2O_3 appear at 500 °C, the intensity of the α-Fe_2O_3 increasing with increasing calcination temperature as the crystallinity increases. Above 600 °C, $AlFeO_3$ appears; this formation temperature is much lower than previously reported [17]. At 1000 °C, the phase transition from γ-Al_2O_3 to α-Al_2O_3 is observed.

The effect of Al_2O_3 additions to Fe_2O_3 is shown in the XRD patterns of the samples calcined at 600 °C (Fig. 1(b)). The 100 mol.% Fe_2O_3 and 90 mol.% Fe_2O_3 samples show strong peaks of α-Fe_2O_3, the intensity of which decreases with increasing Al_2O_3 content. XRD peaks of γ-Fe_2O_3, together with α-Fe_2O_3, also appear in the 60–80 mol.% Fe_2O_3 samples. As the Al_2O_3 content increases further, γ-Al_2O_3 is detected in the 40–50 mol.% Fe_2O_3 samples, while amorphous XRD halos are seen in the 20 mol.% Fe_2O_3 sample. These XRD results indicate that the presence of Al_2O_3 both retards the thermal transformation of γ-Fe_2O_3 to α-Fe_2O_3 and delays the crystallization of iron oxide [18].

A field map of the product phases as a function of composition and heating temperature is shown in Fig. 2. All the as-synthesized samples are amorphous. In the Fe-rich region, γ-Fe_2O_3 is formed at 300–600 °C while α-Fe_2O_3 and $AlFeO_3$ appear >600 °C. In the Al-rich region, γ-Al_2O_3 is formed >500 °C and α-Al_2O_3 >900 °C. Comparison of this field map with that of samples prepared by coprecipitation [18] (Fig. 2) shows several differences. Samples synthesized by the coprecipitation method were amorphous, but all crystallized at 500–700 °C; this crystallization temperature is higher than for the present GE samples. The crystallization temperature increased with increasing Al_2O_3 content in the Fe-rich compositions and was highest at about 60 mol.% Fe_2O_3 composition. Another difference concerns the crystalline product phases; α-Fe_2O_3 but no γ-Fe_2O_3 or $AlFeO_3$ was formed in the Fe-rich samples, while the crystalline phases changed from γ-Al_2O_3 to θ-Al_2O_3 and then to α-Al_2O_3 with increasing temperature in the Al-rich samples. These differences indicate that the synthesis procedure significantly affects the phase formation at different calcination temperatures.

The lattice parameter values of γ-Fe_2O_3 and α-Fe_2O_3, calculated by the least squares method, showed variation corresponding to the compositions. The lattice parameter of γ-Fe_2O_3 (a = 0.8347 nm) of the 100 mol.% Fe_2O_3 sample calcined at 300 °C is in good agreement with the reported value a = 0.8352 nm (ICDD card No. 39–1346). Increasing Al content results in a decrease in the lattice parameter due to the substitution of the smaller Al^{3+} (ionic radius (r) = 0.0535 nm) for Fe^{3+} (r = 0.0645 nm) [19]. As shown in Fig. 3, Al^{3+} ions appear to be incorporated up to about 11–15 mol.% in γ-Fe_2O_3 and about 6–14 mol.% in α-Fe_2O_3. The present results are in fair agreement with the reported data [20–22].

3.2. Effect of alumina on the adsorption ability of the samples

The simultaneous uptake capacities (Q_0) for Ni^{2+}, NH_4^+ and $H_2PO_4^-$ are shown in Fig. 4 as a function of the Fe/(Fe + Al) molar ratios. For Ni^{2+} (Fig. 4(a)), the Q_0 (Ni^{2+}) values range from 1.5 to 2.4 mmol/g. The samples containing 60–80 mol.% Fe_2O_3 clearly show a higher uptake than the other compositions, and the samples heated at 500–600 °C also show a higher uptake than the

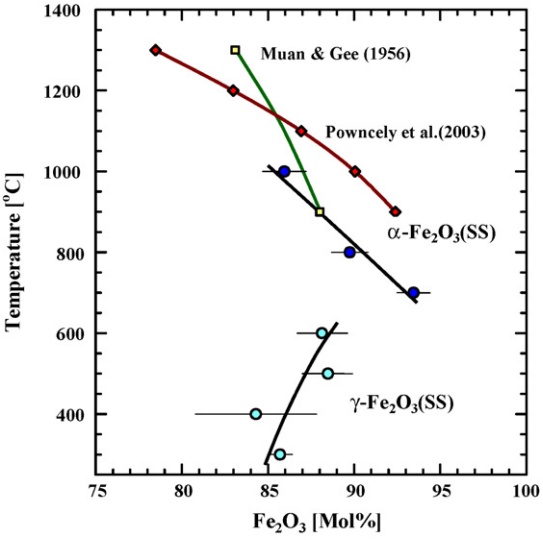

Fig. 3. Solid solution fields of γ-Fe_2O_3 and α-Fe_2O_3 obtained in this work and Refs. [14,15].

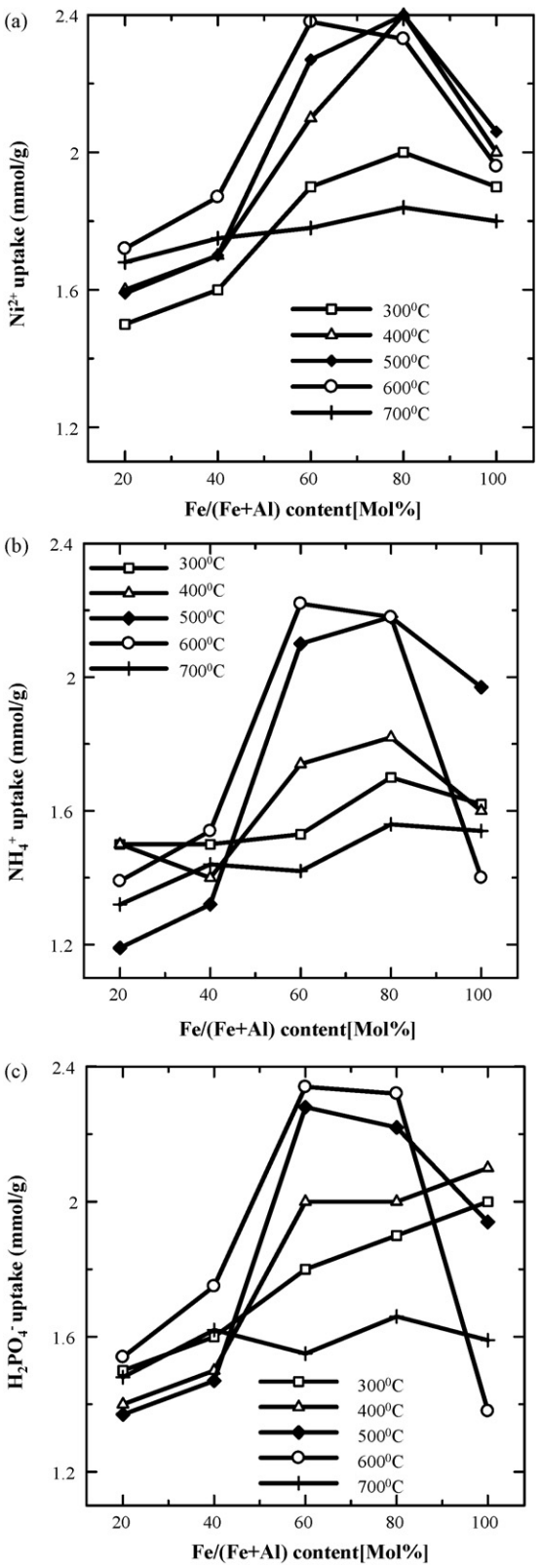

Fig. 4. Simultaneous uptake of ions from solution. (a) Ni^{2+}, (b) NH_4^+ and (c) $H_2PO_4^-$.

samples heated at other temperatures. The Q_0 (NH_4^+) values in Fig. 4(b) range from 1.1 to 2.2 mmol/g. The uptake of NH_4^+ was higher than for Ni^{2+} in the same samples. Fig. 4(c) shows that the Q_0 ($H_2PO_4^-$) values range from 1.2 to 3.7 mmol/g, the samples showing the higher uptakes being same as those showing high Ni^{2+} and

Table 1
Specific surface area (S_{BET}) of samples.

Fe/(Fe + Al) [mol.%]	Calcination temperature [°C]						
	As-syn.	300	400	500	600	700	800
60	10	132	82	48	38	18	9
80	8	157	49	42	23	12	3
100	7	103	26	10	5	<1	<1

NH_4^+ uptakes, but with a different effect of temperature, since the as-synthesized samples showed higher uptake than the calcined samples. This may depend on the surface charge of the adsorbents. The pH values of the as-synthesized samples range from 3.7 to 3.8, at which pH, the surfaces of the samples are positively charged due to the formation of Fe-OH_2^+ and Al-OH_2^+ surface groups in solution. These species will attract negatively charged $H_2PO_4^-$ rather than Ni^{2+} or NH_4^+. The 60–80 mol.% Fe_2O_3 samples calcined at 500–600 °C show higher $H_2PO_4^-$ uptake values than the other calcined samples.

All the Q_0 values for the three ions show similar trends with sample composition and heating temperature. The maximum Q_0 values for Ni^{2+}, NH_4^+ and $H_2PO_4^-$ are almost identical for the three ions (2.4, 2.2 and 2.3 mmol/g, respectively). The uptake of Ni^{2+}, NH_4^+ and $H_2PO_4^-$ by CAS [3] and CFS [4] is in the order $Q_0(NH_4^+) \ll Q_0(H_2PO_4^-) \leq Q_0(Ni^{2+})$, indicating that the present compounds have very good simultaneous uptake abilities for all three ions and show much higher Q_0 values for NH_4^+ than CAS and CFS. The uptake abilities for the three ions increase with increasing heating temperature from 300 to 600 °C though the S_{BET} values decrease significantly (Table 1). Since the pure Fe_2O_3 samples show lower uptake abilities than those of the 80 mol.% Fe_2O_3 samples, incorporation of Al in the Fe_2O_3 appears to play an important role in enhancing the simultaneous uptake of Ni^{2+}, NH_4^+ and $H_2PO_4^-$.

As the crystallinity of the γ-Fe_2O_3 phase improves with increasing calcination temperature, the uptake ability for Ni^{2+}, NH_4^+ and $H_2PO_4^-$ increases. The specific surface area value appears to have little effect on the uptake property. The Fe^{3+} and Al^{3+} concentrations in the solution were below the detection limit in the calcined samples but were detectable in the as-synthesized samples. During the uptake reactions by the present samples, the final pH values range from 4.5 to 5.5 for the calcined samples and 3.7–3.8 for the as-synthesized samples. Since these values do not differ much from the initial pH value, this is an advantage of the present samples because it is not necessary to control the solution pH as were the cases of CAS [3] and CFS [4], increasing the pH by dissolving of Ca^{2+}.

The sorption capacities of the present samples were compared with other reported cost effective sorbents. On phosphate uptake ability, Drizo et al. [23] reported uptake abilities of various sorbents such as expanded vermiculite, natural zeolite, burnt oil shale, baux-

Table 2
Ni^{2+} uptake ability of various samples.

Sample	Uptake capacity [mmol/g]	Refs.
Activated carbon	0.03	[24]
Activated carbon (acid treated)	0.57	[25]
Coir pitch carbon	1.06	[26]
Clay (HCl treated)	0.19	[27]
Clay (untreated)	0.21	[27]
Clay (NaOH treated)	0.25	[27]
Red mud	0.26	[28]
Fly ash	0.01	[29]
Blast furnace slag	0.95	[30]
Amorphous $CaAl_2Si_2O_8$	0.5	[31]
CAS	4.2	[1]
CFS	3.1	[2]
Present compound	2.4	–

Table 3
Saturation magnetization values of the samples.

Fe/(Fe + Al) [mol.%]	Saturation magnetization (M_s) [emu/g]							
	As-syn.	300 °C	400 °C	500 °C	600 °C	700 °C	800 °C	1000 °C
40	<1	1	4	7	10	6	3	<1
50	<1	1	9	17	15	2	2	1
60	<1	17	28	26	18	1	3	1
70	<1	12	36	35	23	1	5	8
80	1	26	46	43	6	2	3	<1
90	1	29	56	47	1	1	1	1
95	1	50	61	36	1	1	1	1
100	1	35	46	1	1	1	1	1

ite, lime stone and fly ash but all of their uptake values were lower than 0.01 mmol/g. Higher uptake abilities were observed in aluminous sorbents of alum (0.03 mmol/g) [24] by substitution for SO_4^{2-} group and γ-alumina (0.33 mmol/g) [25] by amphoteric property and Mg-clays of serpentine (0.092 mmol/g) [26] and palygorskite (0.88 mmol/g) [27], suggesting by formation of Mg-phosphates. Further higher uptake was observed in calcium bearing amorphous compounds such as acid treated slag (1.05 mmol/g) [28] and paper sludge (1.28 mmol/g) [29]. The uptake mechanism of these sorbents is considered to be similar with CAS [3] and CFS [4]. Interesting point of the present compounds is having similarly high phosphate uptake with those sorbents even without CaO component.

Compared with the above mentioned phosphate uptake data, less uptake data have been reported for ammonium ion by cost effective sorbents. This may be due to the presence of many kinds of cation exchangeable materials such as zeolites. The maximum ammonium uptake by the present samples (2.2 mmol/g) is much higher than those reported, e.g. acid treated slag (0.007 mmol/g) [28] and sepiolite (0.1 mmol/g) [30]. The uptake ability is also higher than those of CAS (0.7 mmol/g) [3] and CFS (0.9 mmol/g) [4].

The Ni^{2+} sorption capacities of various sorbents are listed in Table 2. The uptake ability of the present sample is higher than most of the reported cost effective sorbents. However, it is lower than CFS (3.1 mmol/g) [4] and CAS (4.7 mmol/g) [3] due to the lacking of CaO component replacing for Ni^{2+}. Higher uptake of the present samples than activated carbons suggests that local surface charge and/or structural stress by incorporation of Al ion for iron oxide structures may play an important role for enhancement of the uptake ability. Further systematic investigation is, however, necessary to elucidate the uptake mechanisms of the present samples.

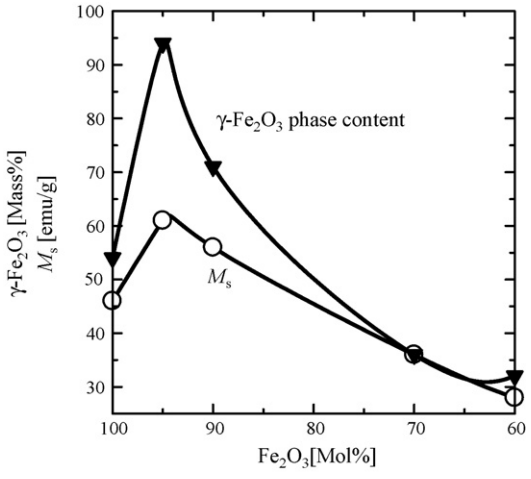

Fig. 5. Saturation magnetization value (M_s) and γ-Fe_2O_3 content as a function of Fe/(Fe + Al) ratio of the samples.

3.3. Effect of alumina on the magnetic properties of the samples

The magnetic properties of the samples were measured to determine their potential usefulness for magnetic separation after adsorption. The magnetization was determined as a function of magnetic field at room temperature by VSM. The saturation magnetization (M_s) values obtained for the samples with different Fe/(Fe + Al) molar ratios and subjected to different calcination temperatures are shown in Table 3. The samples containing γ-Fe_2O_3 show much higher M_s values than those containing α-Fe_2O_3 because γ-Fe_2O_3 is ferrimagnetic while α-Fe_2O_3 is antiferromagnetic or very weakly ferromagnetic [32].

The magnetization values (M_s) for the different samples can be correlated with the presence of γ-Fe_2O_3 determined from the XRD peak intensity, shown in Fig. 5 for the samples heated at 400 °C. The maximum M_s value of 61 emu/g was observed in the 95 mol.% Fe_2O_3 sample, in very good agreement with the maximum γ-Fe_2O_3 content (94 mass%). The γ-Fe_2O_3 contents in the 60 and 70 mol.% Fe_2O_3 samples are only 32 and 36 mass% respectively, and these samples show lower M_s values. The crystal field map of the phases (Fig. 2) shows that the addition of Al_2O_3 to Fe_2O_3 increases the phase transformation temperature of γ-Fe_2O_3 to α-Fe_2O_3 to 600 °C, though this phase transition would normally occur at ≈400 °C [4]. This increase of phase transition temperature (i.e. the stabilization of γ-Fe_2O_3) causes enhancement of γ-Fe_2O_3 content in their samples and increased the sample magnetization, thus, the addition of Al_2O_3 to Fe_2O_3 influences the magnetic property of these Fe_2O_3–Al_2O_3 compounds. It is also clear that the samples in the Fe-rich region containing high γ-Fe_2O_3 contents and showing high M_s values have the advantage of facilitating magnetic separation of the absorbent from solution at the completion of the adsorption process.

4. Conclusion

Fe_2O_3–Al_2O_3 compounds of different Fe/(Fe + Al) molar ratios were prepared by a gel evaporation (GE) method and calcined at 300–1000 °C in air. Their simultaneous uptake abilities for Ni^{2+}, NH_4^+ and $H_2PO_4^-$ were examined and the effect of alumina on the phases formed, adsorption abilities and magnetic properties was also determined, with the following results:

1. The as-synthesized samples were amorphous, but crystallized on heating at 300–600 °C. The addition of Al_2O_3 to Fe_2O_3 suppresses this crystallization and retards the thermal transformation of γ-Fe_2O_3 to α-Fe_2O_3. The lattice parameter values suggest that Al^{3+} is incorporated into these phases up to about 15 mol.% in γ-Fe_2O_3 and 14 mol.% in α-Fe_2O_3.
2. The uptake ability of the samples depends on both the Fe/(Fe + Al) molar composition and calcination temperature and improves with the crystallinity of the γ-Fe_2O_3 phase. The 80 mol.% Fe_2O_3 samples calcined at 500 and 600 °C show the best simultane-

ous uptake of Ni^{2+}, NH_4^+ and $H_2PO_4^-$, illustrating the effect of incorporating Al_2O_3 into Fe_2O_3.

3. The magnetic properties of the samples improve with the addition of Al_2O_3, which increases the γ-Fe_2O_3 content. Samples with good magnetic properties have the advantage of allowing magnetic separation of contaminated adsorbents from solution after uptake.
4. Since the present materials are consisted of ubiquitous and harmless components and show excellent properties for simultaneous uptake of various harmful ions, they are considered to be a good candidate material for removing harmful cations and anions simultaneously from water environments.

Acknowledgements

F. Gulshan thanks the Ministry of Education, Culture, Sports, Science and Technology, Japan for the award of a graduate scholarship (Monbukagakusho Scholarship) under which the present study was carried out. We are grateful to Professor K.J.D. MacKenzie of Victoria University of Wellington for critical reading and editing of the manuscript.

References

[1] K. Okada, Y. Ono, Y. Kameshima, A. Nakajima, K.J.D. MacKenzie, Simultaneous uptake of ammonium and phosphate ions by compounds prepared from paper sludge ash, J. Hazard. Mater. 141 (2007) 622–629.
[2] H. Katsumata, S. Kaneco, K. Inomata, K. Itoh, K. Funasaka, K. Masuyama, T. Suzuki, K. Ohta, Removal of heavy metals in rinsing wastewater from plating factory by adsorption with economical viable materials, J. Environ. Manag. 69 (2003) 187–191.
[3] K. Okada, M. Shimazu, Y. Kameshima, A. Nakajima, K.J.D. MacKenzie, Simultaneous uptake properties of Ni^{2+}, NH_4^+ and PO_4^{3-} by amorphous $CaO–Al_2O_3–SiO_2$ compounds, J. Colloid Interf. Sci. 305 (2006) 229–238.
[4] A. Kobayashi, F. Gulshan, Y. Kameshima, A. Nakajima, K. Okada, Preparation and simultaneous ion uptake properties of $CaO–Fe_2O_3–SiO_2$ compounds, J. Ceram. Soc. Jpn. 116 (2008) 187–191.
[5] M. Rovira, J. Giménez, M. Martínez, X. Martínez-Lladó, J. Pablo, V. Martí, L. Duro, Sorption of selenium(IV) and selenium(VI) onto natural iron oxides: goethite and hematite, J. Hazard. Mater. 150 (2008) 279–284.
[6] M. Biterna, A. Arditsoglou, E. Tsikouras, D. Voutsa, Arsenate removal by zero valent iron: batch and column tests, J. Hazard. Mater. 149 (2007) 548–552.
[7] J. Gimenez, M. Martinez, J. Pablo, M. Rovira, L. Duro, Arsenic sorption onto natural hematite, magnetite and goethite, J. Hazard. Mater. 141 (2007) 575–580.
[8] X. Huang, Intersection of isotherms for phosphate adsorption on hematite, J. Colloid Interf. Sci. 271 (2004) 296–307.
[9] J. Xiong, Z. He, Q. Mahmood, D. Liu, X. Yang, E. Islam, Phosphate removal from solution using steel slag through magnetic separation, J. Hazard. Mater. 152 (2008) 211–215.
[10] N. Boujelben, J. Bouzid, Z. Elouear, M. Feki, F. Jamoussi, A. Montiel, Phosphorus removal from aqueous solution using iron coated natural and engineered sorbents, J. Hazard. Mater. 151 (2008) 103–110.
[11] N.I. Chubar, V.A. Kanibolotskyy, V.V. Strelko, G.G. Gallios, V.F. Samanidou, T.O. Shapo-shnikova, V.G. Milgrandt, I.Z. Zhuravlev, Adsorption of phosphate ions on novel inorganic ion exchangers, J. Colloids Surf. A 255 (2005) 55–63.
[12] S. Tanada, M. Kabayama, N. Kawasaki, T. Sakiyama, T. Nakamura, M. Araki, T. Tamura, Removal of phosphate by aluminium oxide hydroxide, J. Colloid Interf. Sci. 257 (2003) 135–140.
[13] J. Hu, G. Chen, M.C. Irene, Selective removal of heavy metals from industrial wastewater using maghemite nanoparticle: performance and mechanisms, J. Environ. Eng. 7 (2006) 709–715.
[14] F.B. Li, X.Z. Li, C.S. Liu, T.X. Liu, Effect of alumina on photocatalytic activity of iron oxides for bisphenol A degradation, J. Hazard. Mater. 149 (2007) 199–207.
[15] E.A. El-Sharkawy, S.A. El-Hakam, S.E. Samra, Effect of thermal treatment on the various properties of iron (III)–aluminium (III) coprecipitated hydroxide system, Mater. Lett. 42 (5) (2000) 331–338.
[16] S. Vivekanandhan, M. Venkateswarlu, N. Satyanarayana, P. Suresh, D.H. Nagaraju, Munichandraiah, Effect of calcining temperature on the electrochemical performance of nanocrystalline $LiMn_2O_4$ powders prepared by polyethylene glycol (PEG-400) assisted Pechini process, Mater. Lett. 60 (2006) 3212–3216.
[17] A. Muan, On the stability of the phase $Fe_2O_3{\cdot}Al_2O_3$, Am. J. Sci. 256 (1958) 413–422.
[18] F. Gulshan, Y. Kameshima, A. Nakajima, K. Okada, Simultaneous ion uptake properties of $Fe_2O_3–Al_2O_3$ compounds prepared by coprecipitation method, Proc. Waste Eng. (2008) 237–242.
[19] R.D. Shannon, Revised effective ionic radii in halides and chalcogenides, Acta Cryst. A32 (1976) 751–767.
[20] P. Piszora, E. Wolska, X-ray powder diffraction study on the solubility limits in the goethite-diaspore solid solutions, Mater. Sci. Forum 278–281 (1998) 584–588.
[21] A. Muan, C.L. Gee, Phase equilibrium studies in the system iron oxide-Al_2O_3 in air and at 1 atm O_2 pressure, J Am. Ceram. Soc. 39 (1956) 207–214.
[22] M.I. Powncely, K.K. Constantic-Carey, M.J. Fisher-White, Subsolidus phase relationships in the system $Fe_2O_3–Al_2O_3–TiO_2$ between 1000 and 1300 °C, J. Am. Ceram. Soc. 86 (2003) 975–980.
[23] A. Drizo, C.A. Frost, J. Grace, K.A. Smith, Physicochemical screening of phosphate-removing substrates for use in constructed wetland systems, Water Res. 33 (1999) 3595–3602.
[24] M. Ozacar, I.A. Sengil, Enhancing phosphate removal from wastewater by using polyelectrolytes and clay injection, J. Hazard. Mater. B 100 (2003) 131–146.
[25] K. Okada, J. Temuujin, Y. Kameshima, K.J.D. MacKenzie, Simultaneous uptake of ammonium and phosphate ions by composites of γ-alumina/potassium aluminosilicate gel, Mater. Res. Bull. 38 (2003) 749–756.
[26] S. Kaneko, K. Nakajima, Phosphorus removal by crystallization using a granular activated magnesia clinker, J. Water Pollut. Control Fed. 60 (1988) 1239–1244.
[27] H. Ye, F. Chen, Y. Sheng, G. Sheng, J. Fu, Adsorption of phosphate from aqueous solution onto modified palygorskites, Sep. Purif. Technol. 50 (2006) 283–290.
[28] O. Khelifi, Y. Kozuki, H. Murakami, K. Kurata, M. Nishioka, Nutrients adsorption from seawater by new porous carrier made from zeolitized fly ash and slag, Mar. Pollut. Bull. 45 (2002) 311–315.
[29] V.K. Jha, Y. Kameshima, A. Nakajima, K. Okada, K.J.D. MacKenzie, Multifunctional uptake behaviour of materials prepared by calcining waste paper sludge, J. Environ. Sci. Health A41 (2006) 703–719.
[30] M.P. Bernal, J.M. Lopez-Real, Natural zeolites and sepiolite as ammonium and ammonia adsorbent materials, Biores. Technol. 43 (1993) 27–33.
[31] K. Periasamy, C. Namasiviayam, Removal of nickel (II) from aqueous solution and nickel plating industry wastewater using an agricultural waste: peanut hulls, J. Waste Manage. 15 (1995) 63–68.
[32] G. Ennas, G. Marongiu, A. Musinu, A. Falqui, P. Ballirano, R. Caminiti, Characterization of nanocrystalline γ-Fe_2O_3 prepared by wet chemical method, J. Mater. Res. 14 (1999) 1570–1575.